Comparative analysis of CAX2-like cation transporters indicates functional and regulatory diversity

Clare Edmond, Toshiro Shigaki, Sophie Ewert, Matthew D Nelson, James M Connorton, Vesela Chalova, Zeenat Noordally, Jon K. Pittman

Comparative analysis of CAX2-like cation transporters indicates functional and regulatory diversity

Clare Edmond*, Toshiro Shigaki†, Sophie Ewert*, Matthew Nelson*[1], James Connorton*, Vesela Chalova†[2], Zeenat Noordally*[3], Jon K. Pittman*[4]

*Faculty of Life Sciences, University of Manchester, Michael Smith Building, Oxford Road, Manchester, M13 9PT, U.K., and †United States Department of Agriculture/Agricultural Research Service Children's Nutrition Research Center, Baylor College of Medicine, 1100 Bates Street, Houston, Texas 77030, U.S.A.

[1] Present address: School of Biological Sciences, University of Southampton, Bassett Crescent East, Southampton, SO16 7PX, U.K.
[2] Present address: Department of Food Science and Center for Food Safety and Microbiology, University of Arkansas, Fayetteville, AR 72701, U.S.A.
[3] Present address: Biology Department, University of York, York, YO10 5YW, U.K.

[4] To whom correspondence should be addressed (email jon.pittman@manchester.ac.uk)

Short title: CAX2-like cation transporters
Abbreviations used: CAX, cation exchanger; CFP, cyan fluorescent protein; EST, expressed sequence tag; FCCP, carbonyl cyanide *p*-trifluoromethoxy-phenylhydrazone; GUS, β-glucuronidase; MS, Murashige and Skoog; qRT-PCR, quantitative real-time PCR; RACE, rapid amplification of cDNA ends; RT-PCR, reverse transcription-PCR; UTR, untranslated region; YFP, yellow fluorescent protein; YPD, yeast extract-peptone-dextrose

Synopsis
Internal compartmentalisation of metals is an important metal tolerance mechanism in many organisms. In plants and fungi, sequestration into the vacuole is a major detoxification mechanism for metals. Cation transport into the vacuole can be mediated by cation/H^+ exchanger (CAX) transporters. The *Arabidopsis thaliana* AtCAX2 transporter was previously shown to transport Ca^{2+}, Cd^{2+} and Mn^{2+}. To assess the conservation of functional and regulatory characteristics of CAX2-like transporters in higher plants, we have characterized AtCAX2 orthologues from *Arabidopsis* (AtCAX5), tomato (LeCAX2) and barley (HvCAX2). Substrate specificity and regulatory activity was assessed using a yeast heterologous expression assay. Each CAX could transport Ca^{2+} and Mn^{2+} into the yeast vacuole but they each had different cation transport kinetics. Most notably there was variation in the regulation of the transporters. As previously found with AtCAX2, only expression of an N-terminally truncated AtCAX5 in yeast was able to mediate Ca^{2+} and Mn^{2+} transport indicating that activity may be controlled by an auto-regulatory region at the N-terminus. In contrast either full-length or truncated LeCAX2 could efficiently transport Ca^{2+}, although Mn^{2+} transport was controlled by the N-terminus. HvCAX2 did not appear to possess an N-terminal regulatory domain. Expression of *AtCAX2* was not significantly modulated by metal stress; however, *AtCAX5* and *HvCAX2* were transcriptionally up-regulated by high Mn^{2+} treatment, and by Ca^{2+} and Na^+ stress, respectively. It is therefore apparent that despite the high sequence identity between plant *CAX2* orthologues there is significant diversity in their functional characteristics, particularly with regard to regulatory mechanisms.

Key words: *Arabidopsis*, barley, calcium and manganese transport, cation/proton antiporter, regulation, tomato

INTRODUCTION

All organisms have an essential requirement for a wide range of metals, such as various trace metals including Zn^{2+}, Fe^{2+} and Mn^{2+} which function as enzyme co-factors and protein components, and metals like Ca^{2+} that have cell signalling roles. These essential metals are extremely toxic at elevated concentrations and thus many organisms have sophisticated mechanisms to tolerate metal stress. The removal of metals out of the cytoplasm is an important tolerance mechanism. In plants and fungi, the sequestration of metal ions or metal-complexes into the vacuolar compartment is a critical response to metal stress. For example, when yeast (*Saccharomyces cerevisiae*) is deleted for the vacuolar Cd^{2+}-conjugate transporter YCF1 it is extremely sensitive to Cd^{2+} stress [1]. Likewise, the accumulation of excess Ca^{2+} or Mn^{2+} into plant vacuoles can provide tolerance to these stresses [2, 3]. The molecular and biochemical characterisation of such vacuolar sequestration pathways is, however, limited to just a few transporters from a small number of species.

Many ion sequestration pathways utilise the electrochemical proton gradient generated by proton pumps [4]. Higher plants such as *Arabidopsis thaliana* possess a variety of gene families which together encode many putative proton-coupled ion transporters, some of which are predicted to be vacuolar-localised and high-capacity cation transporters [4, 5]. One such gene family is the cation exchanger (CAX) family which has 6 members in *Arabidopsis* and a similar number in rice [6, 7]. *AtCAX1* was identified as a high-capacity, low-affinity Ca^{2+}/H^{+} antiporter from a yeast Ca^{2+} hypersensitivity suppression screen [8] and has subsequently been shown to be involved in Ca^{2+} signalling events and provide tolerance to excess Ca^{2+} [3, 9-11]. AtCAX2 has a lower affinity for Ca^{2+} transport than AtCAX1 [8] and can transport a range of cations into the vacuole, including Mn^{2+} and Cd^{2+} [12-15]. Knockout analysis suggests that AtCAX2 does not have a major physiological role in Ca^{2+} homeostasis but is important for vacuolar Mn^{2+} accumulation [14]. All plant CAX transporters characterised to date appear able to transport Ca^{2+}, but further analysis is needed to determine whether a broad metal substrate range is a common characteristic of CAX proteins.

Other notable features to emerge from the characterisation of *Arabidopsis* CAX transporters are their modes of regulation. *AtCAX1* is expressed at high levels in leaf and flower tissues [16] and is induced by elevated Ca^{2+} [3]. In contrast, *AtCAX2* is detected at fairly low levels in all tissues but is not greatly induced by any metal [12]. AtCAX1 is also regulated post-translationally [17]. A domain on the N-terminal tail of AtCAX1 regulates Ca^{2+} transport activity through an autoinhibitory process [18]. If expressed in yeast or tobacco, full-length AtCAX1 is inactive, while N-terminal truncated or mutated AtCAX1 shows deregulated activity [10, 19]. Interaction with activator proteins or phosphorylation appears to activate AtCAX1 [19, 20]. AtCAX2 is likely to be regulated by a similar manner as it is unable to suppress Ca^{2+} and Mn^{2+} sensitivity of yeast unless it is N-terminally truncated [14, 21]. There is some evidence that CAX transporters from other plants are regulated by a similar mechanism [7, 22], however, it is still unclear whether this mode of regulation is ubiquitous amongst plant CAX-type transporters.

Recent phylogenetic analysis has shown that higher plant CAX genes can be clustered into two groups, Type IA and Type IB [6]. The majority of the characterised plant CAX genes to date are from the Type IA group, which includes *AtCAX1*, *AtCAX3, VCAX1* and *OsCAX1a* [16, 23, 24]. The Type IB group includes *AtCAX2* and *OsCAX3* [7]. Our hypothesis is that these two groups of transporters have different functions and characteristics but further evidence is needed to clarify this. It is also unclear how much functional variation exists within each group and whether the characteristics of the *Arabidopsis* genes can be used as a paradigm for orthologous CAX genes from other species within each group. This is important if we wish to effectively utilise the wealth of knowledge gained from the model plant *Arabidopsis* and translate this into economically important crop plant species. The identification of CAX2-like transporters in crops such as rice or barley that can mediate the vacuolar sequestration of essential metal nutrients will be attractive candidates for

future plant improvement studies to generate plants with improved nutritional content. We have therefore focused further analysis on the characterisation of *AtCAX2*-related genes. In this report, we have characterised plant *CAX2*-like cDNAs including an *Arabidopsis* homologue of *AtCAX2* termed *AtCAX5*, and identified two orthologous cDNA clones from a solanaceous dicot plant, tomato (*LeCAX2*) and the monocot cereal barley (*HvCAX2*). Analysis of the substrate specificity and regulatory characteristics of these related transporters suggests while some characteristics are conserved amongst *CAX2*-like genes, there is still significant variation in the function of members of this CAX Type IB phylogenetic clade.

EXPERIMENTAL

Plant and yeast material

Arabidopsis thaliana (accession Col-0) was grown at 22°C in 18h light on solid one-half strength (0.5×) Murashige and Skoog (MS) medium or on soil. Tomato (*Lycopersicon esculentum* cv. Microtom) and barley (*Hordeum vulgare* cv. Maris Otter) were grown on soil under glasshouse conditions. Barley seedlings were also grown on 0.5× MS plates. For metal stress-treatments, *Arabidopsis* plants grown on 0.5× MS plates for 2 weeks or barley seedlings grown on 1× MS medium for 2 weeks were transferred to 0.5× MS medium containing the metal salt and incubated for 12 h until the tissue was harvested. For AtCAX6::GUS (β-glucuronidase) analysis, transgenic *Arabidopsis* generation and histochemical GUS assay were performed as described [14]. The *S. cerevisiae* strain K667 (*cnb1*::*LEU2 pmc1*::*TRP1 vcx1*Δ) [25] was used for heterologous expression using the yeast expression vector p2HGpd. Yeast transformation and growth analysis was carried out as described [13]. Protein was isolated from yeast and western blotting performed as described [22]. YFP (yellow fluorescent protein) and CFP (cyan fluorescent protein) tagged CAX proteins expressed in yeast were visualised by confocal and epifluorescence microscopy using Leica SP5 and DMR microscopes (Leica Microsystems) and an argon laser with standard YFP and CFP excitation and emission wavelengths (for confocal) or YFP and CFP filter cubes (Chroma Technology) for epifluorescence. The fluorescent yeast vacuole marker stain carboxy-DCFDA (5-(and 6-)carboxy-2',7'-dichlorofluorescein diacetate) [26] was detected using a L4 FITC filter cube.

Plasmid DNA constructs

The full-length and truncated *AtCAX2* cDNA constructs were generated previously [13, 14]. The *AtCAX5* cDNA was identified as an expressed sequence tag (EST) clone (accession number BG459283, obtained from Prof. C. Benning, Michigan State University). The primers sCAX5FOR and CAX5REV (see Table S1 for primer sequences) were used to amplify the *sAtCAX5* cDNA encoding N-terminal truncated AtCAX5. Full-length *AtCAX5* was amplified using CAX5FOR and CAX5REV. *sAtCAX5* and *AtCAX5* were cloned into pGEM-T Easy (Promega) for sequencing. Intron 5 was removed from *sCAX5* and *AtCAX5* by PCR mutagenesis [27] using CAX5Mut primers. *sAtCAX5* and *AtCAX5* were subcloned into the *Xba*I and *Not*I sites of p2HGpd. To generate an N-terminal YFP-AtCAX2 fusion, *EYFP* cDNA (Clontech) amplified using YFPFOR and YFP/CFPREV, was cloned into the *Bam*HI-*Nco*I sites of *AtCAX2* (amplified using CAX2tagFOR with CAX2REV [14]). To generate an N-terminal CFP-AtCAX5 fusion, *ECFP* cDNA (Clontech) amplified using CFPFOR and YFP/CFPREV, was cloned into the *Xba*I-*Nco*I sites of *AtCAX5* (amplified using CAX5tagFOR and CAX5REV). Both constructs were subcloned into p2HGpd. To generate *AtCAX6-GUS*, the 0.8 kb promoter fragment of *AtCAX6* was amplified using primers CAX6PROMF and CAX6PROMR and transcriptionally fused to *GUS* by subcloning into the modified pBI121 plasmid [14]. Barley EST sequences (including EST accession numbers AV834864 and AV910358) were identified with high sequence identity to the 5′ and 3′ ends of *AtCAX2*. The primers HvCAX2FOR and HvCAX2REV amplified *HvCAX2* cDNA from barley root and leaf RNA by RT-PCR (reverse transcription-PCR). *HvCAX2* was cloned into pGEM-T Easy

(Promega) for sequencing then sub-cloned into p2HGpd. *HvCAX2* cDNA was also obtained from a barley embryo cDNA library (from Dr C. Bray, University of Manchester) using a PCR-based cDNA screening method [28]. 5′-RACE (rapid amplification of cDNA ends) was performed using a RACE kit (Roche) and the gene specific primers HvCAX2SP1 and HvCAX2SP2. A barley cDNA clone designated "CAX" (accession number AB218888) identified by *HvCAX2* BLAST search was identical at the amino acid level to *HvCAX2* cDNA. A C-terminal tagged sAtCAX2-c-Myc fusion protein was generated previously [13]. *HvCAX2-c-Myc* was generated using the same method by cloning the *c-Myc* sequence into *HvCAX2* amplified using HvCAX2FOR and HvCAX2tagREV. Various tomato EST sequences with high identity to 5′ and 3′ ends of *AtCAX2*, and an unnamed full-length cDNA sequence (accession number BT014476) with high sequence identity to *AtCAX2* were identified by BLAST. The primers LeCAX2FOR and LeCAX2REV amplified *LeCAX2* cDNA by RT-PCR from tomato leaf RNA. *LeCAX2* was cloned into pGEM-T Easy (Promega) for sequencing then sub-cloned into p2HGpd. N-terminally truncated *sLeCAX2* was amplified using sLeCAX2FOR and LeCAX2REV.

RNA extraction and cDNA amplification

RNA was isolated from *Arabidopsis*, barley and tomato tissues using an RNA extraction kit (Qiagen) and DNase-treated prior to RT-PCR using SuperScriptII reverse transcriptase (Invitrogen) and an oligo dT primer. Expand (Roche) DNA polymerase (for *Arabidopsis* and tomato) or Phusion (Finnzymes) DNA polymerase with GC buffer (for barley) were used with PCR conditions: 94°C for 2 min then 40 cycles of 94°C for 30 sec, 60°C for 1 min, 72°C for 2 min, for the amplification of all full-length cDNA. *Arabidopsis* and barley quantitative *CAX* transcript expression was performed by qRT-PCR (quantitative real-time PCR) using a qPCR SYBR Green kit (Eurogentec) and an ABI 7000 detection system (Applied Biosystems). As an internal standard, actin (*ACT2*) primers for *Arabidopsis* (AtACT2F, AtACT2R) or barley (HvACTF, HvACTR) were used. *AtCAX2* primers (AtCAX2F, AtCAX2R) were designed using 3′ untranslated region (UTR) sequence and the *AtCAX5* (AtCAX5F, AtCAX5R) and *AtCAX6* (AtCAX6F, AtCAX6R) primers were designed using 5′ UTR sequence. *HvCAX2* primers (HvCAX2F, HvCAX2R) were designed against the ORF.

Preparation of membrane vesicles and transport analysis

Vacuolar-enriched membrane vesicles were prepared from yeast as described [18]. Time-dependent 10 μM $^{45}CaCl_2$ uptake measurements into membrane vesicles were performed as described [9]. The 200 μM $MnCl_2$-dependent acridine orange fluorescence recovery assay was performed as described [29], except using vacuolar-enriched membrane vesicles. Metal competition experiments were performed as described [13], except using vacuolar-enriched membrane vesicles.

RESULTS

Expression of an *Arabidopsis CAX2*-like gene in response to Mn^{2+} stress

Previously we found that vacuolar Mn^{2+}/H^+ antiport activity in the *Arabidopsis cax2* knockout mutant is significantly reduced compared to wild type yet not completely absent, suggesting the presence of additional vacuolar transporters that are responsible for Mn^{2+}/H^+ transport [14]. *Arabidopsis* has two uncharacterised genes which cluster with *AtCAX2* (*At3g13320*) in the Type IB group, named *AtCAX5* (At1g55730) and *AtCAX6* (At1g55720) [6]. These three genes are highly similar to each other (*AtCAX5* is 87% identical to *AtCAX2* and 88% identical to *AtCAX6* at predicted amino acid level) suggesting that they may have similar functions. The expression level of *AtCAX5* and *AtCAX6* in comparison to *AtCAX2* was compared in *Arabidopsis* seedlings. Using qRT-PCR and UTR sequence primers specific to each *CAX* gene, we could show that *AtCAX5* and *AtCAX6* were both expressed but at lower expression levels compared with *AtCAX2* (Figure 1a). Expression of *AtCAX6* was barely detectable, although *AtCAX6* promoter-GUS reporter analysis

and RT-PCR confirmed that *AtCAX6* was expressed at very low levels, predominantly in the leaf petiole (Figures S1a and S1b).

As *AtCAX5* had the highest expression level of the two *AtCAX2*-like genes, this gene was characterised further. We wished to examine the tissue-specific expression pattern of *AtCAX5* and its expression in response to various metal stresses. Like *AtCAX2*, *AtCAX5* was expressed in all tissues, particularly stem and root, but less in leaf (Figure 1b). This expression profile was equivalent to that determined by publicly available microarray analyses. It is important to note, however, that most *Arabidopsis* microarrays cannot differentiate between *AtCAX5* and *AtCAX6*.

Some of the *Arabidopsis* CAX transporters are transcriptionally up-regulated in response to particular metal stress conditions [3]. Although AtCAX2 is able to transport Ca^{2+}, Cd^{2+} and Mn^{2+}, its expression is not induced by these metals [12] (Figure 1c). Expression of *AtCAX5* was induced slightly by Cd^{2+} and Ca^{2+} compared to water control treatment, and significantly following Mn^{2+} treatment (Figure 1c). In contrast, some metal treatments notably excess Zn^{2+} caused a reduction in *AtCAX5* expression. Ca^{2+} depletion yielded a small increase in *AtCAX5* expression while *AtCAX2* was slightly down-regulated by this treatment (Figure 1c).

Ca^{2+} and Mn^{2+} stress tolerance of yeast by *AtCAX5*

An EST cDNA clone for *AtCAX5* was obtained (accession number BG459283) that appeared to be full-length by restriction digest analysis, however, this *AtCAX5* cDNA was not completely spliced as a 102 bp intron (fifth intron) was still present that would cause a truncation of the encoded protein at transmembrane domain 5. The intron was removed by mutagenesis and the 1326 bp cDNA and the predicted amino acid sequence was identical to the predicted sequence annotation of At1g55730. *AtCAX5* was also amplified by RT-PCR from RNA isolated from various *Arabidopsis* tissues. A single transcript was identified in stem and leaf tissue while two bands of approximately 1.3 kb and 1.4 kb in size were amplified from fruit RNA (data not shown). The 1.4 kb band was *AtCAX5* containing intron 5, indicating that both the fully processed *AtCAX5* and the incompletely spliced form is expressed in certain tissues. Whether a truncated protein is expressed from this transcript and has a function is unclear. The AtCAX5 amino acid sequence has significant similarity to AtCAX2 and an equivalent predicted topology with 11 predicted transmembrane spanning domains, a longer loop region between transmembrane spans 6 and 7, which has multiple acidic residues (the acidic motif), and a long hydrophilic N-terminal tail (Figure S2). The 3-amino acid (CAF) Mn^{2+} specificity determinant of AtCAX2, within transmembrane spanning domain 4 [13], is also conserved in AtCAX5, suggesting that it may also transport Mn^{2+}.

Cation/H^+ antiport activity of AtCAX2 is largely undetectable when expressed in yeast unless the N-terminus is truncated [14]. To examine whether AtCAX5 was similarly regulated, the Ca^{2+} and Mn^{2+} hypersensitive yeast mutant K667 was transformed with full-length *AtCAX5* and truncated *AtCAX5* (*sAtCAX5*) in which translation was initiated at Met-43. *AtCAX5* was unable to confer growth on high Ca^{2+} and Mn^{2+} containing media whereas *sAtCAX5* was able to suppress both the Ca^{2+} and Mn^{2+} hypersensitivity of K667 (Figure 2a). In comparison to sAtCAX2, the ability of sAtCAX5 to suppress these metal phenotypes was not as efficient. Growth of sAtCAX5-expressing K667 was weaker on 250 mM $CaCl_2$ and on 10 mM $MnCl_2$ than the sAtCAX2-expressing strain, while growth of the sAtCAX5 strain on 15 mM $MnCl_2$ was extremely weak (Figure S3a). This reduced tolerance efficiency was not due to altered expression level or membrane localisation. N-terminal YFP-AtCAX2 and CFP-AtCAX5 fusions were both localised to the vacuole when expressed in yeast, as shown by the equivalent localisation pattern with the vacuolar marker stain [26] carboxy-DCFDA (Figure S3b), specifically at the vacuolar membrane (Figure 2b).

AtCAX5 confers cation/H^+ antiport activity

To confirm that the AtCAX5-mediated Ca^{2+} and Mn^{2+} tolerance of K667 was due to cation transport activity, vacuolar-enriched membrane vesicles were isolated from sAtCAX5-K667 yeast

and the accumulation of 10 μM $^{45}Ca^{2+}$ was measured. The sAtCAX5 Ca^{2+} transport was H^+-dependent as $^{45}Ca^{2+}$ accumulation was significantly inhibited by the protonophore FCCP (Figure S4). sAtCAX5 Ca^{2+} transport activity was reduced compared to sAtCAX2 (Figure 3a) although the K_m for Ca^{2+} was equivalent for the two truncated transporters (Table 1). sAtCAX5 had a lower V_{max} compared to sAtCAX2. No significant Ca^{2+}/H^+ antiport activity was detectable from yeast expressing full-length AtCAX5, AtCAX2 or vector only (Figure 3a).

Mn^{2+}/H^+ antiport activity of sAtCAX5 was determined by an acridine orange fluorescence quench assay which monitored the Mn^{2+}-dependent dissipation of the proton gradient in vesicles expressing sAtCAX5. Addition of Mn^{2+} dissipated the proton gradient significantly more rapidly in sAtCAX5-expressing membrane vesicles compared to empty vector control vesicles, although at a reduced level compared to sAtCAX2 (Figure 3b). Addition of FCCP or Triton X-100 detergent caused a complete and rapid fluorescence recovery due to loss of proton gradient, while addition of water alone did not give fluorescence recovery (data not shown).

The substrate specificity of sAtCAX5 was further analyzed by competition of $^{45}Ca^{2+}/H^+$ antiport. $^{45}Ca^{2+}/H$ antiport activity was determined in the presence or absence of excess concentrations of non-radioactive metals Ca^{2+}, Mn^{2+}, Cd^{2+}, Zn^{2+}, Ni^{2+} and Co^{2+} (Figure 4). Ca^{2+} and Cd^{2+} significantly inhibited $^{45}Ca^{2+}$ transport by sAtCAX5 to equivalent levels seen with sAtCAX2; however, the degree of inhibition with Mn^{2+} was slightly less with sAtCAX5 than observed with sAtCAX2. Furthermore, no inhibition of $^{45}Ca^{2+}$ transport by Zn^{2+} was observed with sAtCAX5 while $^{45}Ca^{2+}$ transport by sAtCAX2 was significantly inhibited by Zn^{2+} (Figure 4). Ni^{2+} and Co^{2+} did not inhibit Ca^{2+} transport by sAtCAX2 or sAtCAX5.

Identification of barley and tomato *CAX2*-like genes

Sequence information from genomes and EST sequences from a variety of plant species indicates that *CAX2*-like (Type IB) genes are present in most higher plants [6]. To gain insight into the functions of orthologous *CAX2* genes in other plant species, cDNAs were amplified by RT-PCR from barley and tomato by using available cDNA (EST) sequence information. cDNA sequences with high sequence identify to *AtCAX2* were identified by BLAST search and primers were designed to amplify predicted full-length cDNA sequences from barley and tomato tissues. Sequence comparison (Figure S2) and phylogenetic analysis confirmed that these sequences were highly similar to *AtCAX2* and were named *HvCAX2* and *LeCAX2*. *LeCAX2* appeared to be a full-length cDNA which encoded a protein of significant similarity to AtCAX2 and AtCAX5, including a long N-terminal tail (Figure S2). In contrast, *HvCAX2* encoded a protein with significant similarity to AtCAX2 and AtCAX5, but with a much shorter N-terminus. Further screening of a barley embryo cDNA library and the use of 5′ RACE obtained equivalent *HvCAX2* cDNA clones, confirming that *HvCAX2* was not missing any 5′ cDNA sequence and thus did possess a short N-terminus. Both HvCAX2 and LeCAX2 possess the CAF Mn^{2+} determinant motif [13] shared with AtCAX2 and AtCAX5, and an acidic motif region between transmembrane spans 6 and 7 (Figure S2). These sequence characteristics are also shared with the rice orthologue *OsCAX3*. Two additional domains named c-1 and c-2 (Figure S2) which are predicted to function as substrate selectivity filters [30] are highly conserved amongst these CAX2-like genes.

LeCAX2 was expressed at moderately high levels in leaf and fruit of tomato plants (Figure S1c). Similarly, expression of *HvCAX2*, determined by qRT-PCR, showed high *HvCAX2* expression in first leaves and roots of seedlings grown on artificial medium, and high expression in leaves, main shoot, immature spike and seeds, in mature, soil-grown plants (Figure S1d). This expression profile corresponds with that identified from microarray analysis (see details for Contig9559_at at www.genevestigator.ethz.ch). In addition microarray data indicate that *HvCAX2* is expressed highly in the stamen and anther, and in the grain is preferentially expressed in the embryo rather than endosperm. To assess whether *HvCAX2* expression is altered in response to metal stress, barley seedlings were treated with high concentrations of various metal salts and *HvCAX2* expression was

analysed in shoot tissue. No significant change was observed in response to Mn^{2+}, Cd^{2+} or other heavy metals (Figure 5). In contrast, high Ca^{2+} (100 mM) and salt (100 mM NaCl) treatment caused a significant increase in *HvCAX2* expression.

Cation transport activity of HvCAX2 and LeCAX2

HvCAX2 and *LeCAX2* were expressed in the K667 yeast mutant to assess whether metal tolerance could be provided. An N-terminal truncated version of *LeCAX2* (*sLeCAX2*) lacking the first 32 amino acids and with a Met to Glu-33 substitution for translation initiation was also expressed. K667 yeast expressing *HvCAX2* were able to grow on high Ca^{2+}-containing medium (200 mM $CaCl_2$), however, the growth efficiency was reduced compared to *sAtCAX2* yeast (Figure 6a). Both full-length *LeCAX2* and N-terminal truncated *sLeCAX2* could efficiently suppress the Ca^{2+} hypersensitivity of K667 when grown on 200 mM $CaCl_2$, equivalent to that provided by *sAtCAX2*. On high Mn^{2+} medium (3.5 mM $MnCl_2$) *HvCAX2* could provide only relatively weak growth compared to *sAtCAX2* although this was stronger than that mediated by full-length *AtCAX2*. This relatively inefficient Ca^{2+} and Mn^{2+} tolerance activity of HvCAX2 was not due to reduced protein level in the yeast relative to sAtCAX2 (Figure 6b). *LeCAX2* was unable to provide any Mn^{2+} tolerance to K667 yeast, even at low Mn^{2+} concentrations (1.5 mM $MnCl_2$) but this inability was overcome when the N-terminus was removed as *sLeCAX2*-expressing yeast could grow strongly on high Mn^{2+} (Figure 6a).

To confirm that the cation tolerance phenotypes observed in yeast by *HvCAX2* and *LeCAX2* were due to direct transport activity, proton-dependent Ca^{2+} and Mn^{2+} transport activity was measured in vacuolar membrane vesicles isolated from the yeast strains. In comparison to sAtCAX2, HvCAX2 Ca^{2+}/H^+ antiport activity was reduced while LeCAX2 and sLeCAX2 activity was equivalent to that of sAtCAX2 (Figure 7a). Furthermore, Ca^{2+} transport kinetics for LeCAX2, sLeCAX2 and sAtCAX2 were all similar but HvCAX2 had a slightly higher K_m for Ca^{2+} (Table 1). Mn^{2+}/H^+ antiport activity by HvCAX2 was reduced compared to that of sAtCAX2 (Figure 7b). No Mn^{2+} transport activity could be measured for LeCAX2 while activity of sLeCAX2 was equivalent to that of sAtCAX2.

DISCUSSION

In this study we have analysed the *AtCAX2* gene homologues in *Arabidopsis*, barley and tomato. Like AtCAX2, all three transporters were able to suppress the Ca^{2+} and Mn^{2+} tolerance phenotypes of a metal hypersensitive yeast mutant due to Ca^{2+} and Mn^{2+}/H^+ antiport activity. Furthermore, they all provide metal tolerance by vacuolar sequestration of the cations. Our data therefore suggest that the Type IB CAX proteins, including those from monocots and dicots transport both Ca^{2+} and Mn^{2+}, and this is likely to be a conserved trait throughout this group. Despite this overall similarity in function, we have identified variation in the transport kinetics of these transporters, and more notably, significant variation in the regulatory characteristics of these transporters.

Full-length AtCAX2 is not able to confer growth on high Mn^{2+} or Ca^{2+} when expressed in yeast compared to N-terminal truncated versions [14, 21] (Figure 3), suggesting that the N-terminus regulates transport activity rather than cation selectivity. Here we have demonstrated that AtCAX5 and LeCAX2 can similarly provide Mn^{2+} tolerance in yeast only when truncated at their N-termini (Figures 2 and 6). The N-terminus of AtCAX5 also appears to regulate Ca^{2+} transport, although this is not the case for LeCAX2 (see below). This inhibited transport activity of AtCAX2 and AtCAX5 was equivalent to the regulatory mechanism previously found with AtCAX1 whereby the N-terminal domain regulates Ca^{2+} transport activity due to a process of autoinhibition [10, 18, 19]. Auto-regulatory domains have also been observed on plant and mammalian Ca^{2+}-ATPases and H^+-ATPases [31] and are a very effective means to rapidly regulate transport activity. This is important for Ca^{2+} transporters that play a role in Ca^{2+} signalling as rapid activation and deactivation of Ca^{2+}

flux is central to the generation of Ca^{2+} oscillations [32]. The relevance of post-translational regulation of Mn^{2+} transport is unclear. Mn^{2+} is essential for a plant for many physiological functions including for water oxidation during photosynthesis but it is unclear whether Mn^{2+} has a signalling role like that of Ca^{2+} [33]. Analysis of wild type and deregulated AtCAX1 in tobacco [10] and *Arabidopsis* [19] has confirmed that the AtCAX1 regulatory mechanism is functional *in planta*. Further studies are needed to similarly confirm the regulatory mechanisms of Type IB CAXs in plant cells.

This study also suggests that this regulatory mechanism is not fully conserved for all plant CAX transporters. LeCAX2 has significant sequence similarity to AtCAX2 and AtCAX5 including a long N-terminal tail (Figures S2 and 8). It is therefore intriguing that LeCAX2 can efficiently transport Ca^{2+} at the equivalent level of activity as sLeCAX2 (Figures 6 and 7), although Mn^{2+} transport by LeCAX2 does appear to be constrained by the presence of the N-terminus. Based on AtCAX1 studies, the model of activation of transport activity of the N-terminally inhibited CAX transporters is following interaction with an activator protein [20]. These activators appear to be plant specific since none of the full-length *Arabidopsis* CAX transporters studied to date show high activity when expressed in yeast, unless they are mutated or an activator protein is co-expressed. It is possible that LeCAX2 can mediate Ca^{2+} transport in yeast due to activation by a yeast protein. Alternatively, there may be differences in the mechanism by which transport activity is regulated for this protein. Secondary structure prediction of the N-terminus of selected CAX proteins supports this. Four Type IA CAX proteins (AtCAX1, AtCAX3, VCAX1 and OsCAX1a) which show increased Ca^{2+} transport activity when N-terminally truncated [19, 22, 30] have similar N-terminal secondary structure with an equivalent coil-helix-coil structure predicted at the extreme N-terminus (Figure 8). AtCAX2 and AtCAX5 also have predicted coil-helix-coil regions close to the N-terminus, but the predicted secondary structure of LeCAX2 N-terminus is clearly different, indicating that structural characteristics could explain the apparent regulatory differences. Future mutagenesis analysis of this protein region should be able to discern whether this structure does explain the regulatory characteristics of LeCAX2.

HvCAX2 has a much shorter N-terminal tail compared to LeCAX2 and the *Arabidopsis* proteins and is more analogous to the previously cloned Type IB gene *OsCAX3* from rice [7]. PCR analysis suggested that *HvCAX2* is not a partial length cDNA but does indeed encode a protein with a short N-terminus. Full-length HvCAX2 could efficiently transport both Ca^{2+} and Mn^{2+} although activity was reduced compared to sAtCAX2 (Figure 7). Likewise, full-length OsCAX3 can provide tolerance to moderate concentrations of Ca^{2+} and Mn^{2+} in yeast [7]. It will be interesting to see if truncations of HvCAX2 and OsCAX3 increase transport activity. Alternatively, these transporters may be regulated by other means. The yeast vacuolar Ca^{2+}/H^{+} antiporter VCX1 has a short N-terminus with predicted secondary protein structure similar to HvCAX2 and OsCAX3 (Figure 8). VCX1 is negatively regulated by the Ca^{2+}-dependent protein phosphatase calcineurin, apparently at the post-transcription level [25]. Plants do not possess an orthologue of calcineurin but these transporters could conceivably be regulated by a similar manner.

The significant *HvCAX2* transcript induction by high concentration of Ca^{2+} and Na^{+} (Figure 5c) may indicate a role of this transporter in response to these metal stresses. HvCAX2 may provide Ca^{2+} tolerance by Ca^{2+} sequestration. Direct salt tolerance can be mediated predominantly by Na^{+} transporters encoded by *NHX* genes [4], while *CAX* genes may play a more indirect role. Adaptation and tolerance to salt stress in plants is controlled in part by Ca^{2+} signalling pathways. High salt treatment leads to an increase in cytosolic Ca^{2+} levels that are then returned to low resting levels via the efflux of Ca^{2+} from the cytosol such as into the vacuole. Such a role has previously been proposed for the vacuolar Ca^{2+}/H^{+} antiporter AtCAX3 which is induced by Na^{+} and is important for plant salt tolerance [11, 34]. The lack of transcript induction by Mn^{2+} does not rule out HvCAX2 as having a physiological function in Mn^{2+} transport. AtCAX2 is similarly not up-regulated by Mn^{2+} yet is important for vacuolar Mn^{2+} sequestration [14]. *HvCAX2* was found to be expressed highly in

young seedling tissue but also in seed tissue (Figure S1d). The presence of HvCAX2 in barley seeds, particularly in the embryo, suggests that this transporter may be a determinant for Ca^{2+} and/or Mn^{2+} content in this cereal grain. Future analysis of *HvCAX2* barley transgenic lines will be able to examine this further.

This study has provided the first characterisation of *AtCAX5*. Previously we showed by knockout analysis that AtCAX2 provides Mn^{2+} accumulation into the plant vacuole, yet vacuolar Mn^{2+} transport was not completely abolished in *cax2* [14]. AtCAX5 is therefore a good candidate for providing this residual activity. sAtCAX5 had lower Ca^{2+} and Mn^{2+} transport activity than sAtCAX2 (Figure 3) with a reduced Ca^{2+} transport capacity (Table 1). While the competition experiment suggests that sAtCAX2 may be able to transport Zn^{2+}, there was no inhibition of sAtCAX5-mediated $^{45}Ca^{2+}$ transport by either concentration of non-radioactive Zn^{2+} (Figure 4). Thus, despite the significant sequence similarity between AtCAX2 and AtCAX5, there appear to be differences in function. Another clear distinction between AtCAX2 and AtCAX5 was the transcriptional up-regulation of *AtCAX5* in response to Mn^{2+} and Cd^{2+} (Figure 1). This is interesting as very few plant genes have been previously identified with a significant Mn^{2+} induction profile, particularly Mn^{2+} transporters [33]. In addition there was a slight increase in *AtCAX5* transcript following Ca^{2+} depletion, and a reduction in response to excess Zn^{2+}. The relevance of this is unclear but future genetic analysis of *AtCAX5* using mutant plant lines may uncover the physiological function of this cation transporter.

These genes may provide novel tools for future biotechnological manipulation of plants. Ca^{2+} is an essential nutrient, and manipulation of plant Ca^{2+} levels can have dietary advantages [35]. For example, manipulation of the sAtCAX1 Ca^{2+} transporter can be utilised to improve the Ca^{2+} nutrition of carrots by enhancing Ca^{2+} content [36]. Although sAtCAX1 was amenable for the manipulation of carrot, overexpression of sAtCAX1 in tomato induced various deleterious phenotypes due to high vacuolar Ca^{2+} accumulation [37]. Manipulation of endogenous transporters, such as LeCAX1, may be a means to overcome unwanted phenotypes in some crop species. Enhancement of other essential minerals can also improve crop plant traits. While Mn^{2+} deficiency is not a problem in human diets, the manipulation of plant Mn^{2+} homeostasis has applications for improved growth under non-optimal Mn^{2+} conditions [33]. Sequestration of toxic concentrations of Mn^{2+} can provide tolerance to plants grown on high Mn^{2+}-containing soils, such as acidic soils [2, 12, 29]. In addition, the ability of plants to efficiently accumulate Mn^{2+} can alleviate poor growth on Mn^{2+} deficient soils [38]. Higher Mn^{2+} content in seeds can improve plant germination and seedling establishment on Mn^{2+} poor soils, as has been demonstrated with barley seeds [39]. Seed-expressed HvCAX2 may therefore be a good candidate gene for improving seed Mn^{2+} content.

In summary, we have provided biochemical analysis of novel cation transporters from three plant species; *Arabidopsis* and two economically important crop plants. This study demonstrated the ability of these proteins to transport Ca^{2+} and Mn^{2+} and has indicated differential transcriptional and post-translational regulation of transport activity for each transporter. Future characterisation of these genes *in planta* will clarify these functional and regulatory characteristics. This comparative analysis shows that although the study of *Arabidopsis* CAX genes can provide functional information, the variation in related genes from different species is significant.

Acknowledgements

This work was supported by a Biotechnology and Biological Sciences Research Council David Phillips Fellowship (grant number BB/B502152/1) to J.K.P. T.S. was supported by a National Science Foundation grant (number 0209777). We are extremely grateful to the support of Dr Kendal Hirschi (Baylor College of Medicine) in whose lab the initial cloning of *AtCAX5* was performed, and for his comments to the manuscript. We thank Dr Wanda Waterworth and Dr Cliff Bray (University of Manchester) for providing barley seed and a barley cDNA library, and Thurston Heaton at the Firs Experimental Grounds for barley and tomato plant maintenance.

REFERENCES

1 Li, Z. S., Lu, Y. P., Zhen, R. G., Szczypka, M., Thiele, D. J. and Rea, P. A. (1997) A new pathway for vacuolar cadmium sequestration in *Saccharomyces cerevisiae*: YCF1-catalyzed transport of bis(glutathionato)cadmium. Proc. Natl. Acad. Sci. U.S.A. **94**, 42-47

2 Delhaize, E., Kataoka, T., Hebb, D. M., White, R. G. and Ryan, P. R. (2003) Genes encoding proteins of the cation diffusion facilitator family that confer manganese tolerance. Plant Cell. **15**, 1131-1142

3 Hirschi, K. D. (1999) Expression of Arabidopsis *CAX1* in tobacco: Altered calcium homeostasis and increased stress sensitivity. Plant Cell. **11**, 2113-2122

4 Martinoia, E., Maeshima, M. and Neuhaus, H. E. (2007) Vacuolar transporters and their essential role in plant metabolism. J. Exp. Bot. **58**, 83-102

5 Cai, X. J. and Lytton, J. (2004) The cation/Ca^{2+} exchanger superfamily: Phylogenetic analysis and structural implications. Mol. Biol. Evol. **21**, 1692-1703

6 Shigaki, T., Rees, I., Nakhleh, L. and Hirschi, K. D. (2006) Identification of three distinct phylogenetic groups of CAX cation/proton antiporters. J. Mol. Evol. **63**, 815-825

7 Kamiya, T., Akahori, T. and Maeshima, M. (2005) Expression profile of the genes for rice cation/H^+ exchanger family and functional analysis in yeast. Plant Cell Physiol. **46**, 1735-1740

8 Hirschi, K. D., Zhen, R. G., Cunningham, K. W., Rea, P. A. and Fink, G. R. (1996) CAX1, an H^+/Ca^{2+} antiporter from *Arabidopsis*. Proc. Natl. Acad. Sci. U.S.A. **93**, 8782-8786

9 Cheng, N. H., Pittman, J. K., Barkla, B. J., Shigaki, T. and Hirschi, K. D. (2003) The Arabidopsis *cax1* mutant exhibits impaired ion homeostasis, development, and hormonal responses and reveals interplay among vacuolar transporters. Plant Cell. **15**, 347-364

10 Mei, H., Zhao, J., Pittman, J. K., Lachmansingh, J., Park, S. and Hirschi, K. D. (2007) *In planta* regulation of the *Arabidopsis* Ca^{2+}/H^+ antiporter CAX1. J. Exp. Bot. **58**, 3419-3427

11 Zhao, J., Barkla, B. J., Marshall, J., Pittman, J. K. and Hirschi, K. D. (2008) The *Arabidopsis cax3* mutants display altered salt tolerance, pH sensitivity and reduced plasma membrane H^+-ATPase activity. Planta. **227**, 659-669

12 Hirschi, K. D., Korenkov, V. D., Wilganowski, N. L. and Wagner, G. J. (2000) Expression of Arabidopsis CAX2 in tobacco. Altered metal accumulation and increased manganese tolerance. Plant Physiol. **124**, 125-133

13 Shigaki, T., Pittman, J. K. and Hirschi, K. D. (2003) Manganese specificity determinants in the *Arabidopsis* metal/H^+ antiporter CAX2. J. Biol. Chem. **278**, 6610-6617

14 Pittman, J. K., Shigaki, T., Marshall, J. L., Morris, J. L., Cheng, N. H. and Hirschi, K. D. (2004) Functional and regulatory analysis of the *Arabidopsis thaliana* CAX2 cation transporter. Plant Mol. Biol. **56**, 959-971

15 Korenkov, V., Hirschi, K., Crutchfield, J. D. and Wagner, G. J. (2007) Enhancing tonoplast Cd/H antiport activity increases Cd, Zn, and Mn tolerance, and impacts root/shoot Cd partitioning in Nicotiana tabacum L. Planta. **226**, 1379-1387

16 Cheng, N. H., Pittman, J. K., Shigaki, T., Lachmansingh, J., LeClere, S., Lahner, B., Salt, D. E. and Hirschi, K. D. (2005) Functional association of Arabidopsis CAX1 and CAX3 is required for normal growth and ion homeostasis. Plant Physiol. **138**, 2048-2060

17 Pittman, J. K. and Hirschi, K. D. (2003) Don't shoot the (second) messenger: endomembrane transporters and binding proteins modulate cytosolic Ca^{2+} levels. Curr. Opin. Plant Biol. **6**, 257-262

18 Pittman, J. K. and Hirschi, K. D. (2001) Regulation of CAX1, an Arabidopsis Ca^{2+}/H^+ antiporter. Identification of an N-terminal autoinhibitory domain. Plant Physiol. **127**, 1020-1029

19 Pittman, J. K., Shigaki, T., Cheng, N. H. and Hirschi, K. D. (2002) Mechanism of N-terminal autoinhibition in the *Arabidopsis* Ca^{2+}/H^{+} antiporter CAX1. J. Biol. Chem. **277**, 26452-26459

20 Cheng, N. H., Pittman, J. K., Zhu, J. K. and Hirschi, K. D. (2004) The protein kinase SOS2 activates the *Arabidopsis* H^{+}/Ca^{2+} antiporter CAX1 to integrate calcium transport and salt tolerance. J. Biol. Chem. **279**, 2922-2926

21 Schaaf, G., Catoni, E., Fitz, M., Schwacke, R., Schneider, A., von Wiren, N. and Frommer, W. B. (2002) A putative role for the vacuolar calcium/manganese proton antiporter AtCAX2 in heavy metal detoxification. Plant Biol. **4**, 612-618

22 Pittman, J. K., Sreevidya, C. S., Shigaki, T., Ueoka-Nakanishi, H. and Hirschi, K. D. (2002) Distinct N-terminal regulatory domains of Ca^{2+}/H^{+} antiporters. Plant Physiol. **130**, 1054-1062

23 Ueoka-Nakanishi, H., Nakanishi, Y., Tanaka, Y. and Maeshima, M. (1999) Properties and molecular cloning of Ca^{2+}/H^{+} antiporter in the vacuolar membrane of mung bean. Eur. J. Biochem. **262**, 417-425

24 Kamiya, T., Akahori, T., Ashikari, M. and Maeshima, M. (2006) Expression of the vacuolar Ca^{2+}/H^{+} exchanger, OsCAX1a, in rice: Cell and age specificity of expression, and enhancement by Ca^{2+}. Plant Cell Physiol. **47**, 96-106

25 Cunningham, K. W. and Fink, G. R. (1996) Calcineurin inhibits VCX1-dependent H^{+}/Ca^{2+} exchange and induces Ca^{2+} ATPases in *Saccharomyces cerevisiae*. Mol. Cell. Biol. **16**, 2226-2237

26 Roberts, C. J., Raymond, C. K., Yamashiro, C. T. and Stevens, T. H. (1991) Methods for studying the yeast vacuole. Methods Enzymol. **194**, 644-661

27 Shigaki, T. and Hirschi, K. D. (2001) Use of Class IIS restriction enzymes for site-directed mutagenesis: Variations on phoenix mutagenesis. Anal. Biochem. **298**, 118-120

28 Israel, D. I. (1993) A PCR-based method for high stringency screening of DNA libraries. Nucleic Acids Res. **21**, 2627-2631

29 Delhaize, E., Gruber, B. D., Pittman, J. K., White, R. G., Leung, H., Miao, Y. S., Jiang, L. W., Ryan, P. R. and Richardson, A. E. (2007) A role for the AtMTP11 gene of *Arabidopsis* in manganese transport and tolerance. Plant J. **51**, 198-210

30 Kamiya, T. and Maeshima, M. (2004) Residues in internal repeats of the rice cation/H+ exchanger are involved in the transport and selection of cations. J. Biol. Chem. **279**, 812-819

31 Bækgaard, L., Fuglsang, A. T. and Palmgren, M. G. (2005) Regulation of plant plasma membrane H^{+}- and Ca^{2+}-ATPases by terminal domains. J. Bioenerg. Biomembr. **37**, 369-374

32 McAinsh, M. R. and Pittman, J. K. (2008) Shaping the calcium signature. New Phytol. **in press**

33 Pittman, J. K. (2005) Managing the manganese: molecular mechanisms of manganese transport and homeostasis. New Phytol. **167**, 733-742

34 Barkla, B. J., Hirschi, K. D. and Pittman, J. K. (2008) Exchangers man the pumps: Functional interplay between proton pumps and proton-coupled Ca^{2+} exchangers. Plant Signaling and Behavior. **3**, 354-356

35 Hirschi, K. D. (2004) The calcium conundrum. Both versatile nutrient and specific signal. Plant Physiol. **136**, 2438-2442

36 Morris, J., Hawthorne, K. M., Hotze, T., Abrams, S. A. and Hirschi, K. D. (2008) Nutritional impact of elevated calcium transport activity in carrots. Proc. Natl. Acad. Sci. U.S.A. **105**, 1431-1435

37 Park, S., Cheng, N. H., Pittman, J. K., Yoo, K. S., Park, J., Smith, R. H. and Hirschi, K. D. (2005) Increased calcium levels and prolonged shelf life in tomatoes expressing Arabidopsis H^{+}/Ca^{2+} transporters. Plant Physiol. **139**, 1194-1206

38 Pedas, P., Hebbern, C. A., Schjoerring, J. K., Holm, P. E. and Husted, S. (2005) Differential capacity for high-affinity manganese uptake contributes to differences between barley genotypes in tolerance to low manganese availability. Plant Physiol. **139**, 1411-1420

39 Longnecker, N. E., Marcar, N. E. and Graham, R. D. (1991) Increased manganese content of barley seeds can increase grain yield in manganese-deficient conditions. Aust. J. Agric. Res. **42**, 1065-1074

40 Jones, D. T. (1999) Protein secondary structure prediction based on position-specific scoring matrices. J. Mol. Biol. **292**, 195-202

TABLES AND FIGURE LEGENDS

Table 1 Kinetic characteristics of CAX-dependent Ca^{2+}/H^+ antiport activity

Initial rates of ΔpH-dependent $^{45}Ca^{2+}$ uptake into vacuolar membrane vesicles isolated from K667 yeast expressing various *CAX* genes were calculated over a range of Ca^{2+} concentrations from 1 to 100 µM in the presence of protonophore (5 µM FCCP). All Michaelis-Menten kinetic values are means (±S.E.) of 2-3 independent experiments.

Transporter	K_m	V_{max}
sAtCAX2	42.1 ± 8.9 µM	12.8 ± 2.2 nmol min^{-1} mg^{-1}
sAtCAX5	46.7 ± 6.1 µM	7.6 ± 0.8 nmol min^{-1} mg^{-1}
HvCAX2	51.9 ± 3.5 µM	7.4 ± 1.6 nmol min^{-1} mg^{-1}
LeCAX2	36.0 ± 7.1 µM	16.2 ± 1.8 nmol min^{-1} mg^{-1}
sLeCAX2	38.5 ± 11.3 µM	17.8 ± 3.7 nmol min^{-1} mg^{-1}

Figure Legends

Figure 1 Expression of *AtCAX5* in *Arabidopsis* and in response to metal stress

(**a**) Expression level of *AtCAX2*, *AtCAX5* and *AtCAX6* in 2 week old *Arabidopsis* seedlings grown on one half-strength MS growth medium. (**b**) Expression of *AtCAX2* and *AtCAX5* in various tissues of *Arabidopsis*. (**c**) Expression of *AtCAX2* and *AtCAX5* in *Arabidopsis* seedlings in response to different metal stress conditions. RNA was isolated from whole-plant tissue 12 h after treatment with one half-strength MS growth medium alone (basal), supplemented with various metal salts (Ca, 100 mM $CaCl_2$; Cd, 10 µM $CdCl_2$; Co, 1 mM $CoCl_2$; K, 80 mM KCl; Mn, 2 mM $MnCl_2$; Zn, 5 mM $ZnCl_2$; Na, 100 mM NaCl), or prepared with Ca^{2+} omitted (no Ca). In all experiments (**a-c**) expression of each *CAX* gene was determined by quantitative real-time-PCR relative to actin and is shown as % of actin. All data is mean of three or four replicates, error bars indicate S.E.

Figure 2 Suppression of Ca^{2+} and Mn^{2+} hypersensitivity of yeast by N-terminally truncated *AtCAX5*

(**a**) Suppression of Ca^{2+} and Mn^{2+} sensitivity of the *pmc1 cnb vcx1* yeast mutant (K667) by full-length AtCAX2 and AtCAX5 or N-terminally truncated sAtCAX2 and sAtCAX5 transporters. Saturated liquid cultures of K667 containing various plasmids were diluted to the cell densities as indicated and then spotted onto selection medium lacking His (-His) and yeast-extract peptone dextrose (YPD) medium containing 175 mM $CaCl_2$ or 5 mM $MnCl_2$. Yeast growth at 30°C is shown after 3 d. Representative experiments are shown. (**b**) Confocal fluorescence imaging of yeast cells expressing YFP-AtCAX2 and CFP-AtCAX5 demonstrating localisation at the yeast vacuolar membrane.

Figure 3 Ca^{2+} and Mn^{2+} proton-dependent transport activity of AtCAX5
(**a**) Single 10-min time-point measurements of ΔpH-dependent uptake of 10 μM $^{45}Ca^{2+}$ into vacuolar membrane vesicles prepared from K667 yeast expressing *sAtCAX2*, *sAtCAX5*, *AtCAX2*, *AtCAX5* and empty vector. Results are shown following subtraction of the protonophore FCCP background values. All experiments were performed following the establishment of a pH gradient in the presence of the Ca^{2+}-ATPase inhibitor vanadate. Results are the means of three independent experiments. Errors bars indicate S.E. (**b**) Time course of Mn^{2+}/H^+ antiport activity determined as Mn^{2+}-dependent H^+ transport. Acridine orange fluorescence recovery was determined in vacuolar membrane vesicles prepared from K667 yeast expressing *sAtCAX2*, *sAtCAX5* and empty vector, following the establishment of a pH gradient and the addition of 200 μM $MnCl_2$ at time 0 min. Fluorescence recovery is shown as % of fluorescence following addition of Mn^{2+}. Results are the means of three independent experiments. Errors bars indicate S.E.

Figure 4 Substrate specificity of sAtCAX5 compared to sAtCAX2 as determined by competition analysis
ΔpH-dependent uptake of 10 μM $^{45}Ca^{2+}$ into vesicles isolated from sAtCAX2-expressing K667 yeast (**a**) and from sAtCAX5-expressing K667 yeast (**b**). Ca^{2+}/H^+ antiport activity, estimated as the difference between uptake with and without the protonophore (5 μM gramicidin), was measured in the absence (control) or presence of 10 × or 100 × of non-radioactive $CaCl_2$, $MnCl_2$, $CdCl_2$, $ZnCl_2$, $NiCl_2$ or $CoCl_2$ after 10 min. Ca^{2+} uptake values are shown following subtraction of the gramicidin background values and expressed as percentages of the control in the absence of any excess non-radiolabeled metals. The data represent means of two to six replications from three independent membrane preparations, and the bars indicate S.E.

Figure 5 *HvCAX2* expression in response to metal stress
Expression of *HvCAX2* in barley seedlings in response to different metal stress conditions. RNA was isolated from whole-plant tissue 12 h after treatment with one half-strength MS growth medium alone (basal), supplemented with various metal salts (Ca, 100 mM $CaCl_2$; Cd, 10 μM $CdCl_2$; Co, 1 mM $CoCl_2$; Mn, 2 mM $MnCl_2$; Zn, 5 mM $ZnCl_2$; Cu, 0.1 mM $CuCl_2$; Fe, 5 mM $FeCl_2$; Na, 100 mM NaCl). Expression was determined by quantitative real-time-PCR relative to actin and is shown as % of actin. Data is mean of three replicates, error bars indicate S.E.

Figure 6 Suppression of Ca^{2+} and Mn^{2+} hypersensitivity of yeast by *HvCAX2* and *LeCAX2*
(**a**) Suppression of Ca^{2+} and Mn^{2+} sensitivity of the *pmc1 cnb vcx1* yeast mutant (K667) by full-length HvCAX2 and LeCAX2 or N-terminally truncated sLeCAX2 transporters. Suppression was compared with AtCAX2 and sAtCAX2. Saturated liquid cultures of K667 containing various plasmids were diluted to the cell densities as indicated and then spotted onto selection medium lacking His (-His) and yeast-extract peptone dextrose (YPD) medium containing $CaCl_2$ or $MnCl_2$ concentrations as indicated. Yeast growth at 30°C is shown after 3 d. Representative experiments are shown. (**b**) Western blotting of AtCAX2-c-Myc, sAtCAX2-c-Myc and HvCAX2-c-Myc protein isolated from yeast with an anti-c-Myc antibody.

Figure 7 Ca^{2+} and Mn^{2+} proton-dependent transport activity of HvCAX2 and LeCAX2
(**a**) Single 10-min time-point measurements of Ca^{2+}/H^+ antiport activity determined as ΔpH-dependent uptake of 10 μM $^{45}Ca^{2+}$ into vacuolar membrane vesicles prepared from K667 yeast expressing *sAtCAX2*, *HvCAX2*, *LeCAX2*, *sLeCAX2* and empty vector. Results are shown following subtraction of the protonophore (5 μM FCCP) background values. All experiments were performed following the establishment of a pH gradient in the presence of the Ca^{2+}-ATPase inhibitor vanadate. Results are the means of three independent experiments. Errors bars indicate S.E. (**b**) Mn^{2+}/H^+ antiport activity determined as Mn^{2+}-dependent H^+ transport. Acridine orange fluorescence recovery

after 15 min was measured in vacuolar membrane vesicles prepared from K667 yeast expressing s*AtCAX2*, *HvCAX2*, *LeCAX2*, s*LeCAX2* and empty vector, following the establishment of a pH gradient and the addition of 200 µM $MnCl_2$ at time 0 min. Fluorescence recovery is shown as % of fluorescence following addition of Mn^{2+}. Results are the means of three independent experiments. Errors bars indicate S.E.

Figure 8 Comparison of predicted secondary structure of the N-termini of CAX proteins
Secondary structure prediction of N-terminal domains of plant Type IA CAX proteins from *Arabidopsis* (AtCAX1, AtCAX3), mung bean (VCAX1) and rice (OsCAX1a), and of plant Type IB CAX proteins from *Arabidopsis* (AtCAX2, AtCAX5), barley (HvCAX2), maize (ZCAX2), rice (OsCAX2, OsCAX3) and tomato (LeCAX2). All the Type IA proteins shown have previously been shown to be regulated by an N-terminal domain. The *Saccharomyces cerevisiae* Ca^{2+}/H^{+} antiporter ScVCX1 (a Type IF CAX protein) which does not possess an N-terminal regulatory domain is shown for comparison. Amino acid sequence up to the first predicted transmembrane span is shown. Secondary protein structure was predicted using PSIPRED [40]. A single line denotes a coil, a grey cylinder denotes a helix and a grey arrow denotes a strand.

Biochemical Journal Immediate Publication. Published on 24 Oct 2008 as manuscript BJ20081814

Fig 1

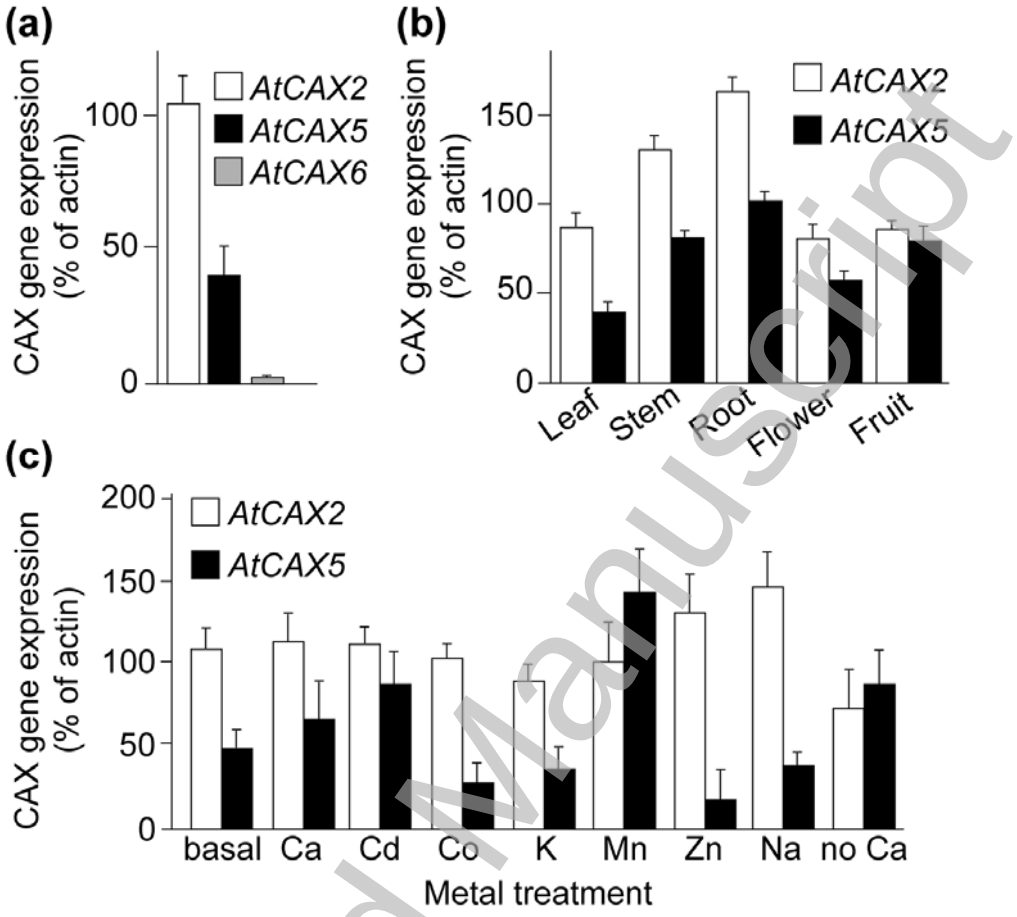

Fig 2

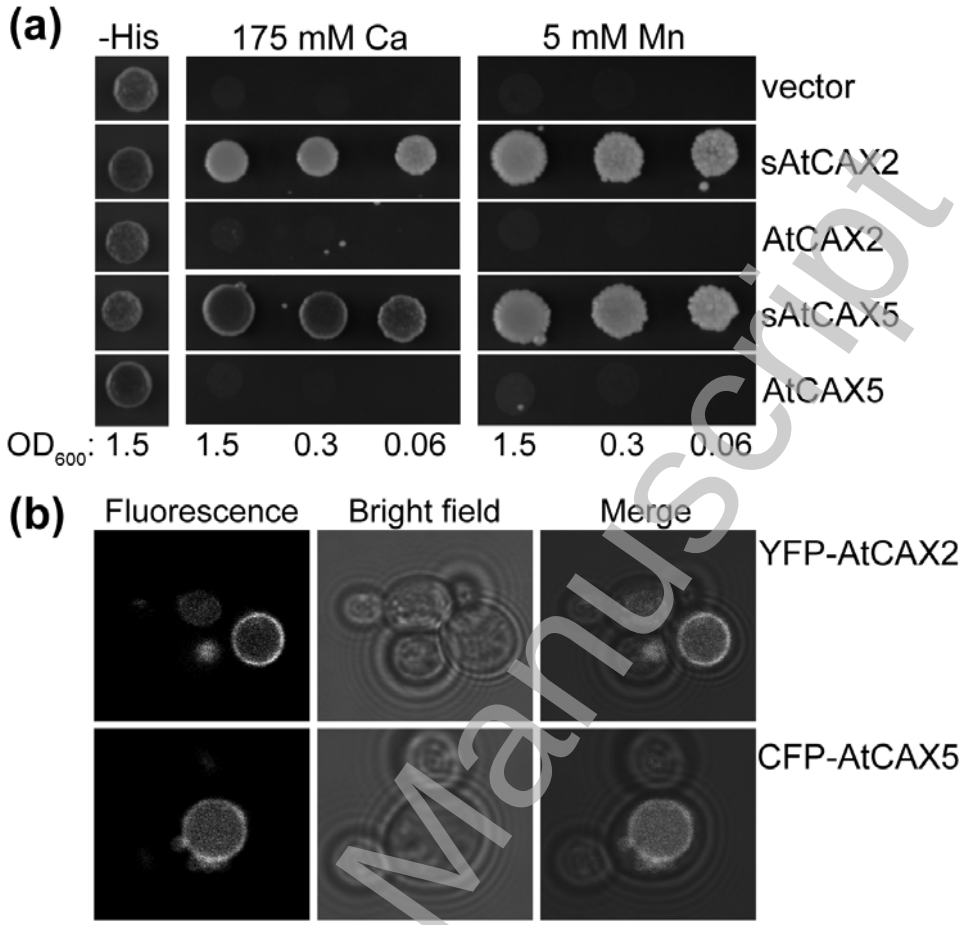

Biochemical Journal Immediate Publication. Published on 24 Oct 2008 as manuscript BJ20081814

Fig 3

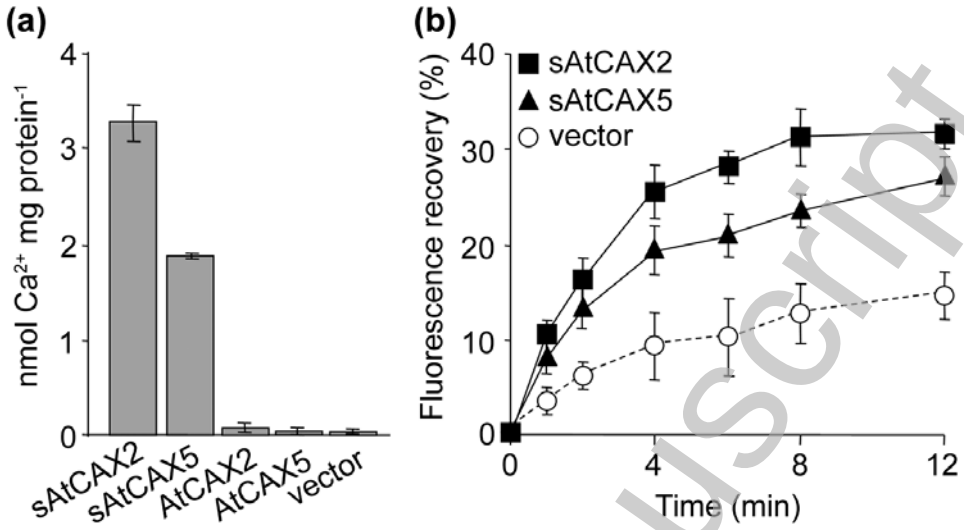

Biochemical Journal Immediate Publication. Published on 24 Oct 2008 as manuscript BJ20081814

Fig 4

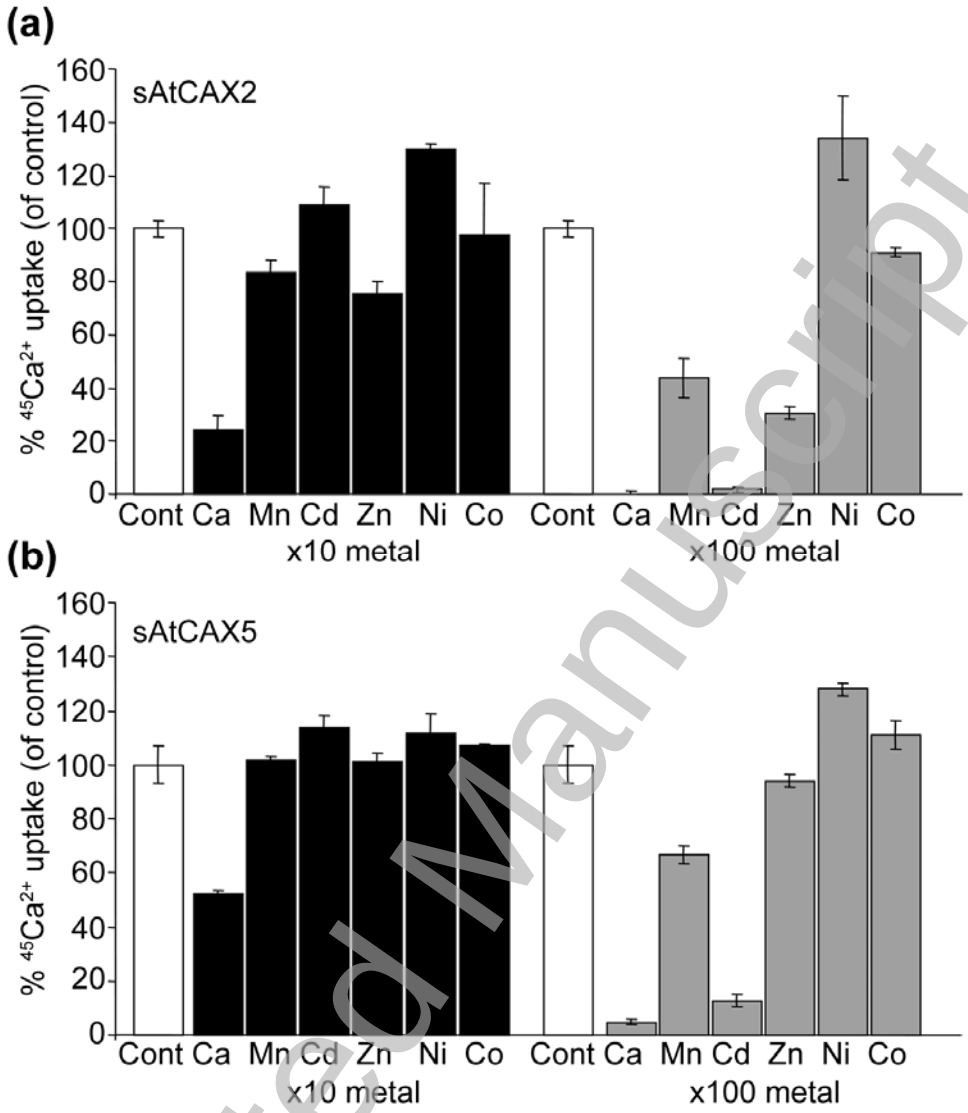

Fig 5

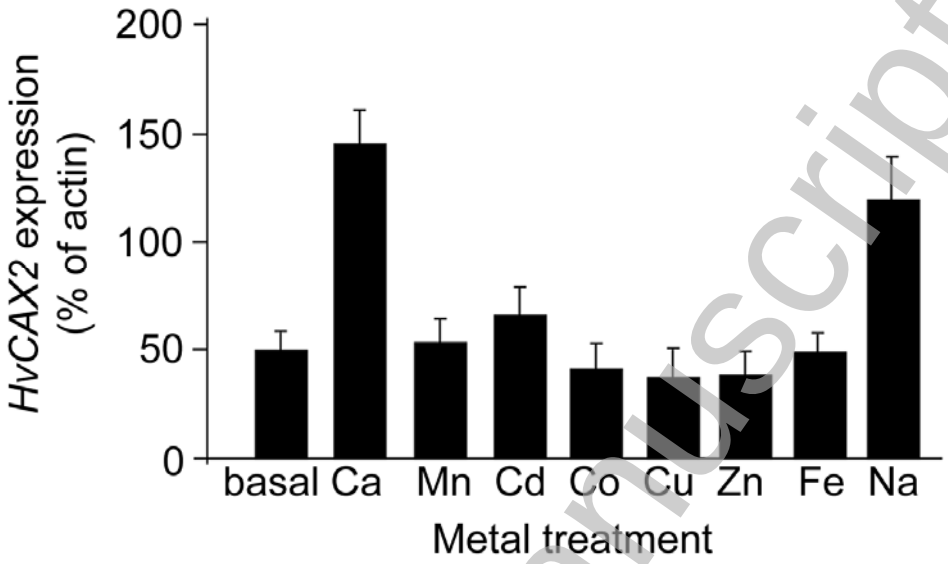

Fig 6

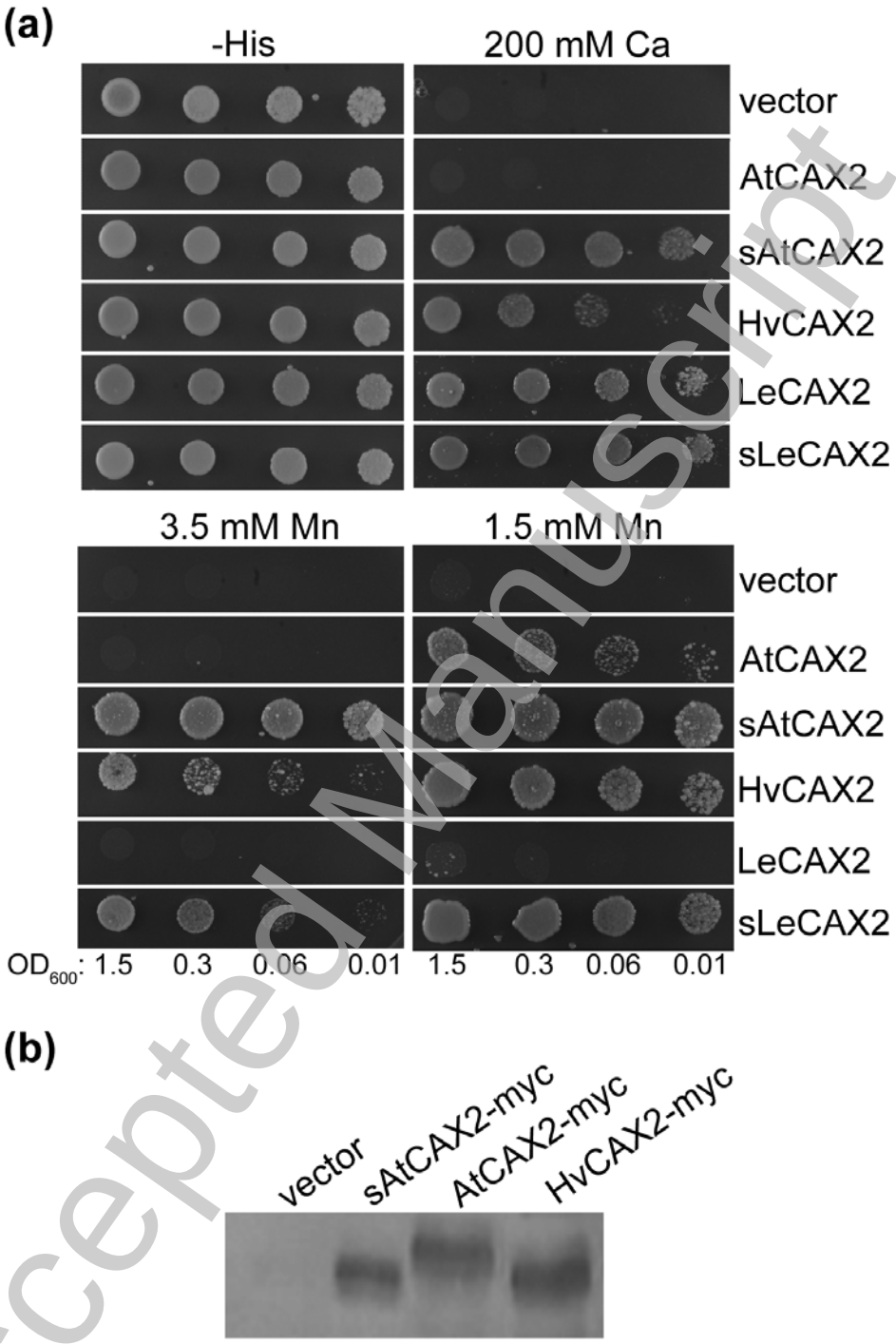

Biochemical Journal Immediate Publication. Published on 24 Oct 2008 as manuscript BJ20081814

Fig 7

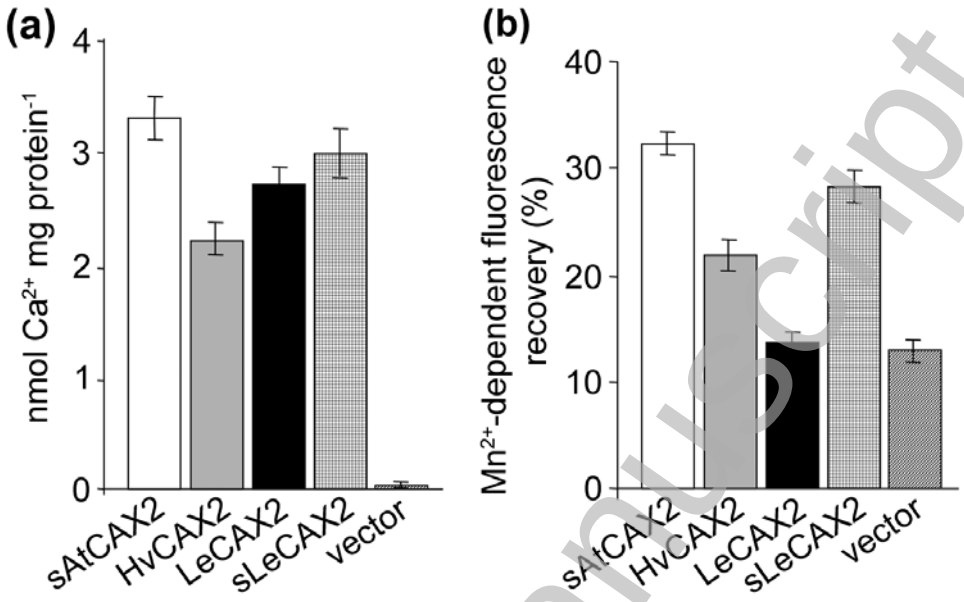

Fig 8